Mitochondrial F-type ATP synthase: multiple enzyme functions revealed by the membrane-embedded FO structure

Mitochondrial F-type ATP synthase: multiple enzyme functions revealed by the membrane-embedded F_O structure

Salvatore Nesci*, Alessandra Pagliarani, Cristina Algieri, Fabiana Trombetti*

Department of Veterinary Medical Sciences, University of Bologna, Ozzano Emilia Via Tolara di Sopra 50, Bologna, 40064, Italy.

*corresponding authors: salvatore.nesci@unibo.it (SN); fabiana.trombetti@unibo.it (FT)

Mitochondrial F-type ATP synthase: multiple enzyme functions revealed by the membrane-embedded F_O structure

Of the two main sectors of the F-type ATP synthase, the membrane-intrinsic F_O domain is the one which, during evolution, has undergone the highest structural variations and changes in subunit composition. The F_O complexity in mitochondria is apparently related to additional enzyme functions that lack in bacterial and thylakoid complexes. Indeed, the F-type ATP synthase has the main bioenergetic role to synthesize ATP by exploiting the electrochemical gradient built by respiratory complexes. The F_O membrane domain, essential in the enzyme machinery, also participates in the bioenergetic cost of synthesizing ATP and in the formation of the *cristae*, thus contributing to mitochondrial morphology. The recent enzyme involvement in a high-conductance channel, which forms in the inner mitochondrial membrane and promotes the mitochondrial permeability transition, highlights a new F-type ATP synthase role. Point mutations which cause amino acid substitutions in F_O subunits produce mitochondrial dysfunctions and lead to severe pathologies. The F_O variability in different species, pointed out by cryo-EM analysis, mirrors the multiple enzyme functions and opens a new scenario in mitochondrial biology.

Keywords: F_1F_O-ATPase; mitochondria; F_O domain; molecular mechanism; structure; membrane

Introduction

Three membrane proteins of rotary ATPase family originating from a common evolutionary ancestor, work as energy transduction complexes in biology. They are identified as: A-, V- and F-type ATPases. A-type ATPases were found in archaea and some bacteria, V-type ATPases are typical of eukaryotic vacuoles, while F-type ATPases occur in eukaryotic mitochondria, chloroplasts and bacteria (Muench et al., 2011). All these rotary ATPases are structurally and functionally similar. The characteristic

hydrophilic and hydrophobic ATPase domains are joined by: a single stalk stator in F-type ATPases; by two stalks and a collar in A-type ATPases and three stalks and a collar in V-type ATPases. The A and F-type ATPases can function as either ATP synthesis or ion pumps, while the V-type ATPases only operate as ATP-driven H^+ pumps (Muench et al., 2011). Interestingly, the two main domains F_1 and F_O in F-type ATPases are basically the ancestral modules found in all rotary ATPases, while the assembling pathway of the F-type mitochondrial enzyme complex (Song et al., 2018) (named ATP synthase or F_1F_O-ATPase) summarizes the phylogeny of the rotary ATPase family. Indeed, the catalytic subunit in the hydrophilic domain F_1 is linked to the central and/or lateral stalks before joining the transmembrane domain F_O (Niu et al., 2017).

The membrane domain of F_1F_O-ATPase, known as F_O, remains the most enigmatic enzyme portion (Boyer, 1997). In all living organisms, the F_1F_O-ATPase is known as the nano-machine that produces ATP, the "molecular energy currency" (Suzuki et al., 2014). The synthesis of ATP in the energy-transducing inner mitochondrial membrane (IMM) is made possible by matching the hydrophobic F_O and hydrophilic F_1 rotary mechanisms, by a structural and functional coupling of the two domains which have different and mutually connected tasks (Junge et al., 1997, 2009).

The protonmotive force (Δp), built by substrate oxidation in the respiratory chain, drives H^+ translocation through F_O domain by generating torque. This torsional mechanism transmitted to the F_1 domain changes the conformations of the catalytic and non catalytic sites to allow ADP phosphorylation. The bi-functional enzyme can also work in *reverse* when the Δp drops and the Gibbs free energy of ATP hydrolysis in F_1 domain powers the H^+ pumping activity of F_O which re-energizes the IMM (Okuno et al., 2011). This reversible energy transduction mechanism, unique in biology, is based on semi-channels, electrostatic barriers, hourglass-shaped rotors and unexpected horizontal

membrane-intrinsic α-helices. The reversible protonation/deprotonation of carboxylic sites not only translocates H^+ across the IMM, but also converts H^+ flux into F_O rotation. The number of proton binding sites varies according to the species and determines the bioenergetic cost of ATP, namely the synthesized ATP molecules per transported H^+, a rotor efficiency parameter. The H^+ pathway through the IMM, which remained enigmatic for decades, can only be defined when considering the F_1F_O-ATPase dynamic structures (Kühlbrandt, 2019).

The F_O subunits also contribute to mitochondrial morphology. Accordingly, supernumerary membrane subunits (SMS) in F_O are involved in supercomplex arrangement and in the IMM ultrastructure. Different SMS participate in the F_1F_O-ATPase dimerization in yeasts and in mammals (Arnold et al., 1998; Gu et al., 2019). The dimers arrange in long rows along the tightly curved IMM ridges, maintain the membrane structure and play a role in mitochondrial bioenergetics (Blum et al., 2019). Conversely, bacterial and chloroplast F_1F_O-ATPases show the minimal subunit composition required for the enzymatic activity and lack SMS, which play a role in membrane plasticity and supramolecular assembly.

Many hints suggest that the enzyme oligomeric arrangement as well as the subunit composition have both functional and structural roles. The recent advances in the elucidation of the F_1F_O-ATPase structure impose a continuous re-evaluation of the enzyme features and roles (Nesci and Pagliarani, 2019). Several aspects remain controversial and the link between structure and function is often not so easy to follow. Most likely, the structural F_1F_O-ATPase arrangement and its role in cellular physiopathology could have more than one answer. The membrane portion F_O, which is still less known than F_1, may still hide intriguing questions to be answered (Nesci et al., 2016).

Overall architecture of mitochondrial F-ATPase(s)

F-type rotary ATPases are hetero-oligomeric membrane-bound enzyme complexes which occur in bacteria, chloroplasts and mitochondria with the same architecture featured by two domains: the chemical nanomotor F_1 and the electrical rotary nanomotor F_O (Junge et al., 2009). The mitochondrial enzyme complex has the most complicated subunit composition (Kühlbrandt, 2019) (Fig. 1). The functional heart of F_1 is an asymmetric hexagonal globular assembly of α and β subunits, arranged as $(\alpha\beta)_3$ around the central γ subunit. This hexamer, in which α and β subunits alternate, hosts three catalytic and three non-catalytic sites. The catalytic sites are located on β subunits at the interface with α subunits. Conversely, the non-catalytic sites occur on the α subunits at the interface with β subunits. The three catalytic β-subunits can adopt three conformations, namely "open", "closed", and "semi-closed", defined as β_E, β_{TP}, and β_{DP}, respectively. The catalytic site β_E is empty, the β_{TP} site hosts Mg·ATP or Mg·ADP, while the β_{DP} site contains Mg·ADP. Each of the three non-catalytic α subunits has a nucleotide site, which only binds Mg·ATP (Hahn et al., 2016). According to the binding change mechanism, the β subunit conformations interconvert each other as the γ subunit rotates (Boyer, 2002). The orientation of γ subunit bulge dictates the momentary conformation of the three catalytic sites and their nucleotide occupancy. Conversely, Mg·ATP bound to the non-catalytic sites allows ADP release from the β_{DP} site and removes the Mg·ADP driven enzyme inhibition during multiple ATP hydrolysis turnover (Murataliev and Boyer, 1992).

The membrane-embedded F_O domain, responsible for H^+ flow across the IMM, shows as signature components the *a* subunit and the c_n-ring, which in turn consists of n subunits arranged as a palisade to form a sort of cylinder. Interestingly, the number of transported H^+ per complete rotation of the the c_n-ring is linked to the number of *c*

subunits, which varies in the range 8-15 among the species. Consistently, the c_n-ring size is tightly related to the ATP bioenergetic cost. Accordingly, the ratio between H^+ translocated and ATP molecules synthesized depends on the number of H^+ binding site(s) on *c* subunits, which varies with the species and is constant in the same species, and the three ATP molecules constantly produced by each β subunit in a complete (360)° rotation of the rotor. In general, an increase in the *c*-ring size implies an increase in the bioenergetic cost of ATP, namely a higher number of H^+ should be translocated from the positive side to negative IMM side to synthetize one ATP molecule. Conversely, small *c* rings are associated with a low bioenergetic cost to synthesize ATP (Pogoryelov et al., 2012). In the oxidative phosphorylation system, Δp, namely the transmembrane thermodynamic force that links substrate oxidation to ADP phosphorylation to yield ATP, has two components: $\Delta\Psi$ (membrane potential difference) and ΔpH (pH gradient) between the mitochondrial matrix and the intermembrane space. During evolution, living organisms have adapted the *c*-ring size to fulfil the requirements of the prevailing electrochemical parameter ($\Delta\Psi$ or ΔpH). Accordingly, when $\Delta\Psi$ is the prevailing driving force accompanied by a low pH gradient, F_O shows a small *c*-ring (von Ballmoos et al., 2008). Apparently, the marine mussel *Mytilus galloprovincialis* shows the same working mode of mammalian F_1F_O-ATPases, namely a small *c* ring associated with a prevailing $\Delta\Psi$ (Nesci et al., 2013).

Conversely, a large *c*-ring is typical of species in which the chemical gradient ΔpH overwhelms the electrical gradient $\Delta\Psi$ (von Ballmoos et al., 2008). In this case more H^+ should be transported across the membrane, because the difference in H^+ concentration between the two membrane sides is the most important parameter to generate the Δp. Moreover, the mitochondrial membrane domain F_O has a different subunit composition in yeast and mammals. Yeast *c*-ring contains ten *c*-subunits (Symersky et al., 2012) as in

bacteria (*E. coli*), while mammalian *c*-ring only contains eight *c*-subunits (Gu et al., 2019).

Some differences among species also exist in the subunit assembly. The mitochondrial F_1F_O-ATPase has a complex structure that consists of different subunits and recruits SMS especially on the F_O domain. Conversely, bacterial and chloroplast F_1F_O-ATPases exhibit a simplified structure in which the *c*-ring, *a* and *b* subunits form the minimal functional assembly.

The minimal functional F_O composition in mitochondria is supplemented by A6L, *e*, *f*, *g*, *k* subunits and by the mammalian diabetes-associated protein in insulin-sensitive tissue (DAPIT), whose functional orthologue is the *i*/*j* subunit in yeasts. Moreover, mammalian 6.8-kDa proteolipid (6.8PL), absent in yeast, forms a long helix in the middle of the *c*-ring (Fig. 2) (Gu et al., 2019). Most of the membrane subunits are encoded by nuclear genes, while *a*, A6L and *c* subunit (identified also as *6*, *8* and *9* subunit) for yeast F_1F_O-ATPase and only *a* and A6L for the mammalian complex are encoded by the mitochondrial DNA (mtDNA).

Two half-channels for H^+ uptake/release through F_O

The H^+ pathway across the IMM has remained enigmatic for decades and only the implementation of technologies in recent years has allowed to clarify how H^+ flux is made possible. Recent developments of X-ray crystallography and cryo-electron microscopy of F_O domain allowed to identify the cluster of charged and polar amino acid residues in the membrane-intrinsic *a*-*c* subunit interface. These amino acid side chains are especially involved in building the H^+ translocation pathway. Unexpectedly, membrane crossing by H^+ exploits a pathway which forms and is localized along the IMM. Accordingly, two asymmetric aqueous half-channels lie on two long hairpin horizontal α-helices, named

H5 and H6, in the *a* subunit, juxtaposed to the *c* subunits, provide access to the H^+-binding sites in the *c*-ring (Allegretti et al., 2015). This unusual α-helix arrangement in the IMM is conserved and apparently constitutes an essential feature of all rotary A-, F- and V-type ATPases (Kühlbrandt and Davies, 2016) The hairpin structure of *c* subunits spans the IMM forming an hourglass shape, which features the *c*-ring, seen laterally from the membrane side. Since the H^+-binding sites are in the concavity, on the outer C-terminal α-helices of *c* subunits, the orthogonal arrangement of the α-helices of *a* subunit perfectly fits the rotor concavity (Klusch et al., 2017).

Ribbons of F_1F_O-ATPase dimers are lining up on the highly curved rim folding the membrane of the *cristae* (Paumard et al., 2002). Interestingly, the pH value at the edge of the *cristae* is higher than that in the intermembrane space opposing the inner boundary membrane (IBM), so as the local pH gradient along the membrane surface which forms the *cristae* is about 0.5 units. This extremely low pH value suggests that the *cristae* work as H^+ traps, to maintain the Δp generated by the electron transport chain across the IMM (Strauss et al., 2008). Consistently, also membrane potential is higher at the *cristae* than in the IBM (Wolf et al., 2019). When protons are driven through F_O for ATP synthesis, pH is around 7.2 in the lumen or *intracristae* space of the channel. The *c*-ring carboxylate which hosts the H^+-binding site has a standard pK_a in water of 5.0, clearly incompatible with the *c*-ring protonated state required by the rotation which allows ATP synthesis. Therefore, in the luminal channel an amazing molecular strategy is built by intermediate amino acid residues, which make H^+ transfer possible. Accordingly, the *a*Glu-223 residue in yeast ($_y$) and *a*Glu-203 in mammals ($_m$) with *a*His-185_y and *a*His-168_m on H6 and H5 helix hairpin of *a* subunit, respectively (Fig. 3AB), form a conserved pair and act as an intermediate H^+-donor site (Srivastava et al., 2018) to *c*Glu-59_y or *c*Glu-58_m of the *c*-ring. The Glu-Glu and His-Glu interaction establish multiple H-bridges in the membrane half-

channel that change the pK_a of the carboxylic group so as to allow its protonation. Moreover, the H^+ access may be favored by the coordination of a metal ion with *a*His-168_m and *a*His-172_m, which synchronizes the *c*-ring protonation to the rotor rotation (Murphy et al., 2019). On the opposite half-channel, which opens in the matrix side, the *a*Glu-162_y and *a*Glu-145_m on H5 (matrix) helix (Fig. 3CD) restore the original pK_a of *c*Glu so as it becomes an effective H^+-releasing site allowing the *c*-ring deprotonation. Moreover, *a*Arg-176_y in yeast or 159_m in mammals form an electrostatic barrier between the two half-channels so as to prevent any H^+ short circuiting and act as a positive attraction pole for the negatively charged carboxylate of *c*Glu-59_y or Glu-58_m (Mitome et al., 2010).

The aqueous cavity on the luminal side viewed from intra-*cristae* space is made possible by polar residues, namely the C-terminal portion of *f* subunit (on the top) flanked by the N-terminal third TM α-helix of *b* subunit (on the right), the H5 with H6 helixes of *a* subunit (on the bottom) and the loop between helix 3 and helix 4 (on the left). On the other side, the matrix side half-channel is formed by the orthogonal arrangement of *a* subunit H5 helix which joins the C-terminal helix of the *c* subunit in the aqueous cavity (Srivastava et al., 2018).

So, the microenvironment built by appropriate amino acid residues is essential for the function. These observations, coming from the increasing knowledge on the structure of the F_1F_O-ATPase, and especially on its membrane domain, strengthen the link between structure and function and the awareness that every molecular and supramolecular arrangement perfectly fits its specific role.

How H^+ translocation turns into a torque generation

In the last years biochemical and computational data lead to formulate microscopic

models to depict how H^+ translocation through the hydrophobic F_O domain can generate a torque. By an amazing mechanism which exploits the F_O bioarchitecture, a force (Δp) perpendicular to the IMM plane is converted to a vectorial torsional force (T) parallel to IMM plane (Elston et al., 1998). The H^+ binding sites in the *c*-ring during the ion translocation are exposed to two different environments (*i.e.* hydrophilic environment within the half-channels and hydrophobic environment inside the IMM), where they adopt different conformations. In the H^+ locally hydrated luminal half-channel, the carboxylic group of *c*Glu is oriented in an outward-facing open conformation (H^+ un-locked conformation) before protonation and re-orients to an inward-faced closed conformation (H^+ locked conformation), when the *c*-ring H^+ binding site becomes protonated. On the opposite matrix half-channel, the *c*Glu is in a H^+ locked conformation and only adopts an H^+ un-locked conformation after deprotonation. The binding-sites of key carboxylate side chains of *c*-ring embedded in the IMM are always oriented in the so-called H^+ locked conformation, namely in the favoured energy state to enter the IMM (Pogoryelov et al., 2010). Moreover, the neutralization of the *c*Glu carboxylate allows the *c*-ring to rotate as a result of Brownian motion (Junge et al., 1997). The direction of rotation is clockwise when viewed from F_O toward F_1 during the ATP synthesis and counterclockwise during the ATP hydrolysis (Nesci et al., 2015; Vinogradov, 2019; Yoshida et al., 2001).

The high H^+ concentration in luminal half-channel drives the protonation of *c*Glu, where the H^+ binding site from the un-locked conformation rearranges to yield the locked conformation, pushed by Δp to enter the IMM. When an almost entire rotation of the rotor is completed, the *c*Glu reaches the basic half-channel on the matrix side and the low H^+ concentration, associated with the negative charge of the "H^+-releasing site" on H5 helix of *a* subunit, favours the *c*Glu deprotonation by changing the H^+ binding site

conformation to the un-locked form. To ensure the coupling between the H^+ movement and *c*-ring rotation and prevent a futile H^+ shortcut, an essential and conserved *a*Arg-176_y or *a*Arg-159_m acts as electrostatic barrier between the two half-channels (Mitome et al., 2010). Moreover, *a*Arg helps to strip off H^+ from *c*Glu during H^+ translocation, without establishing a salt bridge, which by binding *a* and *c* subunits would impede the rotor rotation. However, the distance of about 4.5Å between the *a*Arg and *c*Glu in the un-locked conformation does not allow any interaction (Hahn et al., 2018). These charge positions make the two half-channels at the *a*/*c*-ring interface spatially offset. Accordingly, the two pathways for entry and exit of H^+ are disconnected in order to adjust the rotation direction of the rotor to Δp (Symersky et al., 2012).

The different conformations in the catalytic subunits of F_1, namely β_E, β_{DP} and β_{TP}, also impose different conformations in the transmembrane domain F_O during rotation. The peripheral stalk contains regions, which insert in both F_1 and F_O domains and are thought to be flexible so as to exhibit coordinated conformational changes during the rotation. The central stalk undergoes torsion during catalysis, but also the *c*-ring shows conformational fluctuations as it is in contact with the *a* subunit which transfers H^+.
Thus, the coupling of energy transduction and H^+ translocation is allowed by a flexible coupling and conformational adaptations of the F_1 and F_O domains (Murphy et al., 2019). The flexible rotor can bend and impose conformational changes within the enzyme proteins, which generate the torsion in a synchronized way. Moreover, the 6.8PL fills the central hole inside the *c*-ring and interacts with it by acting as a mechanical obstacle to stop the enzyme rotation in the inhibited state. The 6.8PL position may be involved in the regulation of F_1F_O-ATPase activity (Gu et al., 2019).

F_1F_O-ATPase dimerization and tetramerization: a prerequisite for IMM morphology

Recent advances show that some F_1F_O-ATPase properties linked to its supramolecular arrangement at the apex of the *cristae* and MICOS (mitochondrial contact site and *cristae* organizing system) complex at *cristae* junctions cooperate to yield *cristae* morphology (Eydt et al., 2017). Accordingly, F_1F_O-ATPase dimers found in rows on the IMM appear to be crucial to form the highly curved ridges of the *cristae* (Davies et al., 2012). Dimeric forms were reported in mitochondria, but not in bacteria and chloroplasts. Interestingly, the dimerization interface in different species has different subunit composition with no apparent homology (Kühlbrandt, 2019). Furthermore, in mitochondria of various species four different types of F_1F_O-ATPase dimers were described. In animals and yeasts (*e.g.* *Bos taurus*, *Sus scrofa domesticus,* and *Saccharomyces cerevisiae*) V-shaped dimers, defined type I dimers, were found, localized on the rim of the *cristae* with an IMM convex curvature of about 90° (Hahn et al., 2016; Strauss et al., 2008). Type II dimers of *Polytomella* sp. Pringsheim 198.80 are represented by V-shaped F_1F_O-ATPase dimers that form a 56°angle between the two central stalks, where an extrinsic proteins of unknown evolutionary origin, named ATP Synthase-Associated (*ASA*) subunits, form a robust peripheral stalk (Blum et al., 2019; Klusch et al., 2017). The type III dimers found in *Paramecium multimicronucleatum* are U-shaped with parallel monomers and the two peripheral stalks laterally offset. Even if the dimer angle is close to zero, the dimers can generate the helical tubular *cristae* (Mühleip et al., 2016). Mitochondrial F_1F_O-ATPases that form type IV dimers, found in *Euglena gracilis* and *Trypanosoma brucei*, have been poorly explored. In this case the two central stalks form a similar angle to type II dimers, but they are arranged side by side in parallel as in type III dimers (Mühleip et al., 2017). Mammalian F_1F_O-ATPases can also form a tetramer, in turn formed by the assembly of

two dimers that lie antiparallel to each other, joined by two IF1, an endogenous protein inhibitor (Gu et al., 2019).

The IF_1 is evolutionary conserved throughout all eukaryotes and only blocks ATP hydrolysis without affecting the forward enzyme function of ATP synthesis. Most likely IF1 is not important for cell survival under normal conditions, but can be crucial under pathological or stress conditions (Faccenda et al., 2013). The overexpression of IF1 in some cancer types would be at least partially responsible for the decrease in oxidative phosphorylation which features cancer cells (Esparza-Moltó and Cuezva, 2018). However IF1 not only prevents ATP dissipation by the reverse reaction of F_1F_O-ATPase, but has other crucial functions including a structural role to yield mitochondrial morphology (García et al., 2006; Gu et al., 2019; Nakamura et al., 2013). The active IF_1 dimer, at acidic pHs in the matrix forms from the dissociation of the tetrameric form and prevents ATP hydrolysis when Δp collapses. In the tetramer IF1 is associated with two F_1 domains of two opposite dimers by binding to the catalytic interface between the αDP and βDP subunits in loose binding conformation. Therefore, the two monomers of the laterally opposite dimer share the same IF1 and the two IF1 prevent ATP hydrolysis by a ratchet-like action on the rotor and stabilize the tetramer (Gu et al., 2019).

The F_1F_O-ATPase dimers are also kept together in rows by a long-range attractive force that arises from the relief of the overall elastic strain of the IMM (Anselmi et al., 2018). Nevertheless, the H-shaped tetrameric structure of the mammalian F_1F_O-ATPase, consists of two adjacent type I dimers bound by subunit–subunit interactions, other than by interactions with IF1 dimers (Gu et al., 2019; Nesci and Pagliarani, 2019). The arrangement of the membrane subunits is crucial to allow the interactions within the enzyme dimers and tetramers. In general, the four monomers of each tetramer with their own subunits participate in the building of the contact sites allowing the tetramer

formation. In the F_1F_O-ATPase tetrameric forms, the dimer pairs are linked by interaction sites above the IMM. The dimer-dimer interactions involve both *k* and *b* subunits of two adjacent monomers from two different dimers and *g*-*g* subunit interactions established between opposite monomers of different dimers (OMDD). Furthermore, the interactions between *e*-*e* subunits of OMDD form the tetramer core within the IMM. Accordingly, two dimerization contact sites in mammalian F_1F_O-ATPase V-shaped type I dimers form between *g*/*f* subunits on one side and the DAPIT/*k* subunits on the other side of the same F_1F_O-ATPase monomer. Finally, these dimers are joined to DAPIT/*k* subunits and *g*/*f* subunits, respectively on the opposite monomer of each dimer (Gu et al., 2019).

Differently, in yeasts the *a*, *i*/*j*, *e* and *k* subunits hold the F_1F_O-ATPase dimer by forming tree point of contact between monomers. In the middle of the dimer, at the interface between two F_O domains, two dimerization motifs occur. The former motif is formed by *a* subunits and the latter by the *i*/*j* subunits of each monomer. The dimerization motifs of each monomer connect the dimer to the matrix by *a* subunits, while the dimerization motif of *i*/*j* subunits forms in the *intracristae* space. Noteworthy, these double strand planar structures at the interface of the dimer on *a* subunit and DAPIT orthologs are not present in the mammalian enzyme. Finally, the α helices connections extended to the lumen between *e* and *k* subunits from different monomers contribute, on both dimer sides, to join the two monomers (Guo et al., 2017). However, pioneering studies showed that the physical association of F_O domains depend on the occurrence of *e* and *g* subunits and on a putative conserved dimerization *GxxxG* motif localized in the transmembrane α-helices of both subunits (Arselin et al., 2003; Bustos and Velours, 2005). The substitution of a glycine residue by leucine into the *e* subunit motif led to the loss of *g* subunit and destabilized the dimeric F_1F_O-ATPsynthase structure by causing the concomitant appearance of an anomalous onion-like structure in the *cristae* (Arselin et

al., 2003). An essential role in the cohesion of monomers was highlighted by *e* an *g* subunits. Indeed, disulfide cross-links between *e*-*g* or *e*-*e*/*g*-*g* increased the stability of F_1F_O-ATPsynthase dimers and oligomers, respectively in mitochondrial digitonin extracts (Bustos and Velours, 2005).

Even if the supramolecular F_1F_O-ATPase arrangement directly stems from protein-protein interactions, not all these interactions are involved in IMM bending. However, the curved structure at the apex of the *cristae* arises from unusual bridge-shaped interactions among *e*, *g* subunits, and the N-terminal helix of *b* subunits, as found in yeasts and mammals (Gu et al., 2019; Guo et al., 2017). This arrangement is reminiscent of a BAR-like domain that preferentially bends the lipid bilayer to the highly curved and negatively charged membranes (Peter et al., 2004) to form the apex of *cristae*.

Finally, the F_1F_O-ATPase ultrastructural organization, in which monomer pairs form dimers, dimer pairs form tetramers, which in turn assemble in long rows to form oligomers, shows that subunit–subunit interactions, which join the enzyme monomers, also force the IMM to maintain its convexity at the apex of the *cristae*. The IMM architecture undergoes a physiological age-dependent change and the typical rim shape of the *cristae* disappears when F_1F_O-ATPase dimers dissociate into monomers. Consistently, a deep modification of mitochondrial morphology is produced, including a progressive vesiculation of the IMM, which ultimately leads to mitochondrial dysfunction and cell death (Daum et al., 2013).

F_1F_O-ATPase oligomers safeguard mitochondrial functions

Recently, the dimeric form of F_1F_O-ATPase has been implicated in the mitochondrial permeability transition pore (mPTP), a large pore in the IMM, which makes the membrane permeable to ions and other solutes and triggers cascade events that lead to

cell death (Giorgio et al., 2013). As far as we are aware, the involvement of F_1F_O-ATPase in the mPTP and especially its structural participation in the mechanism of mPTP formation and opening are still a matter of debate. Many hints strongly sustain the hypothesis that the F_1F_O-ATPase, when activated by Ca^{2+}, which replaces the natural cofactor Mg^{2+} when Ca^{2+} concentration increases, is part of or even coincides with the mechanism which opens the mPTP (Baines and Gutiérrez-Aguilar, 2018; Nesci et al., 2018). Accordingly, when the Ca^{2+}-activated F_1F_O-ATPase is inhibited by various compounds, the mPTP formation is delayed or even prevented (Algieri et al., 2019).

The IMM could be depolarized by any increase in conductance upon mitochondrial Ca^{2+} overload, due to transmembrane channels and/or transporters, already described (Carroll et al., 2019; Karch et al., 2019; Mnatsakanyan et al., 2019; Neginskaya et al., 2019; Urbani et al., 2019). Moreover, in this scenario, the F_1F_O-ATPase in monomeric (Alavian et al., 2014) or dimeric form (Giorgio et al., 2013) would contribute to the membrane depolarization by inducing the largest mPTP pore. Accordingly, even if many other mitochondrial channels/transporters house smaller sub-conductance activities, which contribute to the mPTP (Szabo and Zoratti, 2014), most likely they do not represent the main responsible for IMM depolarization. As far as we are aware, the mitochondrial F_1F_O-ATPase is the most likely candidate as high-conductance major channel mPTP, which is inhibited by cyclosporin A (CsA) but not by bongkrekate (BKA) (Mnatsakanyan et al., 2019; Urbani et al., 2019). Additionally, the adenine nucleotide translocase isoforms could form a second low-conductance mPTP inhibited by both CsA and BKA (Karch et al., 2019; Neginskaya et al., 2019).

Noteworthy, the mPTP activity can be enhanced by Ca^{2+} and pharmacologically modulated by selective inhibitors of F_1 (Algieri et al., 2019) and F_O domain (Bonora et al., 2017; Mnatsakanyan et al., 2019; Morciano et al., 2018). Newly, purified and

functionally active F_1F_O-ATPase in monomeric (Mnatsakanyan et al., 2019) and dimeric form (Urbani et al., 2019) acts as a voltage-gated ion channel which exhibits mPTP-like properties. Thus, mechanistic insights in the structural/conformational F_1F_O-ATPase changes are required to understand how the mPTP opens and closes, since the mechanism is apparently reversible. Interestingly, some clues strongly suggest that Ca^{2+}-activated F_1F_O-ATP(hydrol)ase may trigger the mPTP formation by a cascade of conformational events that would involve the IMM chemical-physical properties including lipid composition and membrane curvature (Nesci, 2018; Nesci et al., 2018). The F_O domain features the primary conductance of mPTP, thus suggesting that the channel can form in the F_1F_O-ATPase monomeric/dimeric state (Mnatsakanyan et al., 2019; Urbani et al., 2019). In this context, the *a*, *b*, *c*, *e* and *g* subunits, all membrane subunits, are the main candidates to form the high-conductance channel (Bonora et al., 2013; Carraro et al., 2018; Niedzwiecka et al., 2020).

The most striking opposition to the hypothesis that the F_1F_O-ATPase complex or some F_1F_O-ATPase subunits may be involved in the mechanism of mPTP formation comes from reports in cells in which the structurally defective or vestigial F_1F_O-ATPase lacks the *a* subunit, *c*-ring, OSCP and A6L subunit and consequently cannot translocate H^+. In these cells the mPTP formation was still detectable and CsA-sensitive (He et al., 2017a, 2017b). Lastly, in the clonal cell line HAP1-Δ(*c*+δ), lacking both *c* and δ subunits, the mitochondrial and nuclear-encoded enzyme subunits cannot properly associate, the enzyme complex is defective, but the mPTP is still detected, even if it does not show high conductance activity (Carroll et al., 2019).

However, these data cannot rule out a putative structural involvement of the F_1F_O-ATPase in the mPTP as an alternative explanation can be provided. It seems clear that the failed ATP synthase assembly or the absence of *e* and *g* subunits (Carraro et al., 2018)

deeply alters the mitochondrial morphology and the formation of the *cristae*. This condition can be mimicked by the intact enzyme when Ca^{2+} promotes conformational changes in *e* and *g* subunits, which would prevent both the ATP synthase oligomerization and IMM bending. If the IMM at the tips of *cristae* cannot bend, the membrane curvature decreases and the mPTP opens.

Moreover, the involvement of F_1F_O-ATPase in the mPTP is also strengthened by the report that in aging cells the dissociation of F_1F_O-ATPase dimers leads to mitochondrial dysfunction since changes in the IMM permeability are incompatible with the correct function of the mitochondrial respiratory chain (Di Lisa and Bernardi, 2005).

Most likely, the reversible dissociation of F_1F_O-ATPase dimers hides the key which triggers mPTP formation and mitochondrial dysfunctions.

Structural consequences of amino acid changes in F_O subunits leading to mitochondrial pathologies

While mutations in the nuclear genes which encode F_1F_O-ATPase subunits are rare and associated with diseases nearly incompatible with life, the most known mutations, associated with diseases whose severity is related to mitochondrial heteroplasmy (Uziel et al., 1997), are localized in the mtDNA which encodes two F_1F_O-ATPase subunits, *a* and 8. Accordingly, in mammals mtDNA is known to have a higher mutational rate than nuclear DNA (Jonckheere et al., 2012). The most frequent mutations in the ATP synthase associated with human diseases are in the mitochondrial ATP6 gene, which encodes *a* subunit, which allows H^+ flux within the IMM. Specific amino acids, which reversibly anchor and channel H^+ along their transmembrane route, are required. Several point mutations have been described (Dautant et al., 2018) and their number is fated to increase.

As far as we are aware, the most severe mutation is the m.T8993>G transversion, where the substitution of thymine by guanine results in a missense mutation (*a*Leu156Arg) (Trounce et al., 1994). The clinical phenotype belongs to severe pathologies known as Neuropathy, Ataxia and Retinitis Pigmentosa (NARP) or Maternally Inherited Leigh Syndrome (MILS), whose severity and classification depend on the heteroplasmy degree (Uziel et al., 1997). Since the missense mutation is localized near the crucial electrostatic barrier of *a*Arg-159, the presence of two positive guanidine groups at short distance from each other reduces the H^+ flux across the membrane (Xu et al., 2015) and, consequently also the ATP synthesis. This transversion mainly causes a severe energy deficiency, because the F_1F_O-ATPase cannot work in reverse to pump H^+ and re-energize the IMM. However, the two enzyme domains F_1 and F_O remain structurally and functionally joined. Accordingly, the sensitivity to oligomycin, the selective inhibitor that blocks H^+ flux within F_O, which witnesses the coupling of the two domains, is maintained (Sgarbi et al., 2006).

Another mutation in the mitochondrial ATP6 gene associated with NARP and MILS diseases consists in the m.T9176>G transversion on position 220 of *a* subunit which changes a conserved leucine into arginine (*a*Leu220Arg) (Dautant et al., 2018). Since the *a*Leu-220 is near the essential *a*Arg-159, this transversion implies the occurrence of two close Arg residues whose steric hindrance and electrostatic repulsions destabilize the *a* subunit. Accordingly, the two vicinal Arg would create a positive barrier, which blocks H^+ flux and consequently decreases ATP synthesis and complex IV respiration. Moreover, since ATP hydrolysis becomes uncoupled to proton translocation, as shown by oligomycin insensitivity, the F-ATPase activity cannot pump H^+ and build the membrane potential (Kucharczyk et al., 2019). These two transversions imply the

replacement of a hydrophobic amino acid (Leu) by a basic and positively charged amino acid (Arg), which dramatically changes the microenvironmental features of the protein.

A milder pathological phenotype is caused by m.T8993>C transition, which results in Leu156Pro substitution (Kucharczyk et al., 2009). This m.T8993>C transition increases ROS production, even if allows the maintenance of a slow rotation of the *c*-ring, which couples H^+ flux to a low ATP synthesis (Baracca et al., 2007; Solaini et al., 2008). Most likely proline insertion in replacement of leucine modifies the protein secondary structure, due to the proline 5-membered ring which causes a kink in the helices (Schmidt et al., 2016) and makes H^+ flux difficult.

Myopathy, Lactic Acidosis, and Sideroblastic Anemia (MLASA) is a rare mitochondrial pathology, which has been recently associated with a *de novo* transition (m.G8969>A) in mtDNA which encodes the *ATP6* gene (Burrage et al., 2014). The missense mutation Ser148Asn in *a* subunit of MLASA patients (Skoczeń et al., 2018) is localized at one helix turn from the "H^+ transfer group" *a*Glu-145 in the aqueous half-channel which opens in the mitochondrial matrix (Srivastava et al., 2018). The positive charge of *a*Asn-145 establishes electrostatic bonds with *a*Glu-145 and prevents the H^+ translocation which depends on the –COOH deprotonation of *c*Glu-59 (Skoczeń et al., 2018).

In cancer, some mtDNA point mutations seem to favour tumorigenesis, and other mutations would promote cancer metastasis, while mtDNA depletion correlates with poor prognosis in certain cancer types (Moro, 2019). Mutations that were shown to accumulate in some cancer types, although in yeast models, have been introduced in subunit a of yeast; these recent experiments may cast light on the molecular mechanisms of cancer proliferation. The two mutations *a*Pro153Ser and *a*Lys80Glu (*a*Pro136Ser and *a*Lys64Glu in humans) are associated with carcinogenesis. Most likely, these mutations

make cancer cells refractory to apoptosis because they inhibit the formation of the mPTP in the IMM (Niedzwiecka et al., 2018). Proline substitutions by point mutations decrease the helix packing (Schmidt et al., 2016), while the replacement of Lys by Glu dramatically changes the polarity and acid–base properties of the microenvironment. Most likely the *a*Pro153Ser and *a*Lys-80Glu mutants have a distorted *a* subunit (Niedzwiecka et al., 2018), which would prevent the formation of the mPTP between the two F_O monomers.

To sum up, the mutations in *a* subunit block or hamper the torque generation in F_O, which is essential for the ATP synthesis by F_1 and/or prevent the formation of the mPTP. Mutations in *8* subunit associated with diseases are much less frequent than that in *a* subunit. The mutation Trp55X, where X is a stop codon, implies the shortening of 14 amino acids from the C-terminus of *8* subunit, which destabilizes the enzyme complex. A mutation in the overlapping region of *a* subunit and *8* subunit results in a Thr55Arg replacement in *8* subunit and a met1Thr replacement in *a* subunit, which cause a decrease in F_1F_O-ATP synthase activity in human fibroblasts (Xu et al., 2015).

Cancer and aging share an increased frequency of mutations. The accumulation of mutations which alter the mitochondrial bioenergetics is at the basis of the mitochondrial theory of aging: mtDNA point mutations and deletions are known to accumulate with age in human tissues. Moreover, the occurrence of large mtDNA deletions has been reported as a driver of premature aging (Moro, 2019). Most likely, the age-related increase in mutations that alter the mitochondrial morphology, bioenergetics and lead to mPTP dysregulation (Paradies et al., 2013), involve F_O components.

Conclusion

The mitochondrial F_1F_O-ATPase is now emerging as key enzyme complex in a variety of cell events, including proliferation and death. The membrane sector F_O, even

if not directly involved in catalysis, not only hosts the rotary mechanism driven by H^+ flux, which allows ATP synthesis/hydrolysis, but also rules the mitochondrial shape, the formation of the lethal channel mPTP and the related interplay between supramolecular structures. The F_O subunits and their amino acid composition, which drive the protein conformations and interactions with membrane lipids, are built and assembled according to their precise role(s).

Declaration of interest

This work was financed from CARISBO Foundation grants n° 2018/0375 (AP) and n° 2019.0534 (SN), Bologna, Italy.

Disclosure statement

The authors report no conflict of interest.

ORCID

Salvatore Nesci http://orcid.org/0000-0001-8569-7158

Fabiana Trombetti http://orcid.org/0000-0003-1611-8727

Alessandra Pagliarani http://orcid.org/0000-0002-0604-4587

References

Alavian, K.N., Beutner, G., Lazrove, E., Sacchetti, S., Park, H.-A., Licznerski, P., Li, H., Nabili, P., Hockensmith, K., Graham, M., et al. (2014). An uncoupling channel within the c-subunit ring of the F1FO ATP synthase is the mitochondrial permeability transition pore. Proc. Natl. Acad. Sci. U.S.A. *111*, 10580–10585.

Algieri, C., Trombetti, F., Pagliarani, A., Ventrella, V., Bernardini, C., Fabbri, M., Forni, M., and Nesci, S. (2019). Mitochondrial Ca2+ -activated F1 FO -ATPase hydrolyzes ATP and promotes the permeability transition pore. Ann. N. Y. Acad. Sci. *1457*, 142–157.

Allegretti, M., Klusch, N., Mills, D.J., Vonck, J., Kühlbrandt, W., and Davies, K.M. (2015). Horizontal membrane-intrinsic α-helices in the stator a-subunit of an F-type ATP synthase. Nature *521*, 237–240.

Anselmi, C., Davies, K.M., and Faraldo-Gómez, J.D. (2018). Mitochondrial ATP synthase dimers spontaneously associate due to a long-range membrane-induced force. J. Gen. Physiol. *150*, 763–770.

Arnold, I., Pfeiffer, K., Neupert, W., Stuart, R.A., and Schägger, H. (1998). Yeast mitochondrial F1F0-ATP synthase exists as a dimer: identification of three dimer-specific subunits. EMBO J. *17*, 7170–7178.

Arselin, G., Giraud, M.-F., Dautant, A., Vaillier, J., Brèthes, D., Coulary-Salin, B., Schaeffer, J., and Velours, J. (2003). The GxxxG motif of the transmembrane domain of subunit e is involved in the dimerization/oligomerization of the yeast ATP synthase complex in the mitochondrial membrane. Eur. J. Biochem. *270*, 1875–1884.

Baines, C.P., and Gutiérrez-Aguilar, M. (2018). The still uncertain identity of the channel-forming unit(s) of the mitochondrial permeability transition pore. Cell Calcium *73*, 121–130.

von Ballmoos, C., Cook, G.M., and Dimroth, P. (2008). Unique rotary ATP synthase and its biological diversity. Annu Rev Biophys *37*, 43–64.

Baracca, A., Sgarbi, G., Mattiazzi, M., Casalena, G., Pagnotta, E., Valentino, M.L., Moggio, M., Lenaz, G., Carelli, V., and Solaini, G. (2007). Biochemical phenotypes associated with the mitochondrial ATP6 gene mutations at nt8993. Biochim. Biophys. Acta *1767*, 913–919.

Blum, T.B., Hahn, A., Meier, T., Davies, K.M., and Kühlbrandt, W. (2019). Dimers of mitochondrial ATP synthase induce membrane curvature and self-assemble into rows. Proc. Natl. Acad. Sci. U.S.A.

Bonora, M., Bononi, A., De Marchi, E., Giorgi, C., Lebiedzinska, M., Marchi, S., Patergnani, S., Rimessi, A., Suski, J.M., Wojtala, A., et al. (2013). Role of the c subunit of the FO ATP synthase in mitochondrial permeability transition. Cell Cycle *12*, 674–683.

Bonora, M., Morganti, C., Morciano, G., Pedriali, G., Lebiedzinska-Arciszewska, M., Aquila, G., Giorgi, C., Rizzo, P., Campo, G., Ferrari, R., et al. (2017). Mitochondrial permeability transition involves dissociation of F1FO ATP synthase dimers and C-ring conformation. EMBO Rep. *18*, 1077–1089.

Boyer, P.D. (1997). The ATP synthase--a splendid molecular machine. Annu. Rev. Biochem. *66*, 717–749.

Boyer, P.D. (2002). Catalytic site occupancy during ATP synthase catalysis. FEBS Lett. *512*, 29–32.

Burrage, L.C., Tang, S., Wang, J., Donti, T.R., Walkiewicz, M., Luchak, J.M., Chen, L.-C., Schmitt, E.S., Niu, Z., Erana, R., et al. (2014). Mitochondrial myopathy, lactic acidosis, and sideroblastic anemia (MLASA) plus associated with a novel de novo

mutation (m.8969G>A) in the mitochondrial encoded ATP6 gene. Mol. Genet. Metab. *113*, 207–212.

Bustos, D.M., and Velours, J. (2005). The modification of the conserved GXXXG motif of the membrane-spanning segment of subunit g destabilizes the supramolecular species of yeast ATP synthase. J. Biol. Chem. *280*, 29004–29010.

Carraro, M., Checchetto, V., Sartori, G., Kucharczyk, R., di Rago, J.-P., Minervini, G., Franchin, C., Arrigoni, G., Giorgio, V., Petronilli, V., et al. (2018). High-Conductance Channel Formation in Yeast Mitochondria is Mediated by F-ATP Synthase e and g Subunits. Cell. Physiol. Biochem. *50*, 1840–1855.

Carroll, J., He, J., Ding, S., Fearnley, I.M., and Walker, J.E. (2019). Persistence of the permeability transition pore in human mitochondria devoid of an assembled ATP synthase. Proc. Natl. Acad. Sci. U.S.A. *116*, 12816–12821.

Daum, B., Walter, A., Horst, A., Osiewacz, H.D., and Kühlbrandt, W. (2013). Age-dependent dissociation of ATP synthase dimers and loss of inner-membrane cristae in mitochondria. Proc. Natl. Acad. Sci. U.S.A. *110*, 15301–15306.

Dautant, A., Meier, T., Hahn, A., Tribouillard-Tanvier, D., di Rago, J.-P., and Kucharczyk, R. (2018). ATP Synthase Diseases of Mitochondrial Genetic Origin. Front Physiol *9*, 329.

Davies, K.M., Anselmi, C., Wittig, I., Faraldo-Gómez, J.D., and Kühlbrandt, W. (2012). Structure of the yeast F1Fo-ATP synthase dimer and its role in shaping the mitochondrial cristae. Proc. Natl. Acad. Sci. U.S.A. *109*, 13602–13607.

Di Lisa, F., and Bernardi, P. (2005). Mitochondrial function and myocardial aging. A critical analysis of the role of permeability transition. Cardiovasc. Res. *66*, 222–232.

Elston, T., Wang, H., and Oster, G. (1998). Energy transduction in ATP synthase. Nature *391*, 510–513.

Esparza-Moltó, P.B., and Cuezva, J.M. (2018). The Role of Mitochondrial H+-ATP Synthase in Cancer. Front Oncol *8*, 53.

Eydt, K., Davies, K.M., Behrendt, C., Wittig, I., and Reichert, A.S. (2017). Cristae architecture is determined by an interplay of the MICOS complex and the F1FO ATP synthase via Mic27 and Mic10. Microb Cell *4*, 259–272.

Faccenda, D., Tan, C.H., Seraphim, A., Duchen, M.R., and Campanella, M. (2013). IF1 limits the apoptotic-signalling cascade by preventing mitochondrial remodelling. Cell Death Differ. *20*, 686–697.

García, J.J., Morales-Ríos, E., Cortés-Hernandez, P., and Rodríguez-Zavala, J.S. (2006). The inhibitor protein (IF1) promotes dimerization of the mitochondrial F1F0-ATP synthase. Biochemistry *45*, 12695–12703.

Giorgio, V., von Stockum, S., Antoniel, M., Fabbro, A., Fogolari, F., Forte, M., Glick, G.D., Petronilli, V., Zoratti, M., Szabó, I., et al. (2013). Dimers of mitochondrial ATP

synthase form the permeability transition pore. Proc. Natl. Acad. Sci. U.S.A. *110*, 5887–5892.

Gu, J., Zhang, L., Zong, S., Guo, R., Liu, T., Yi, J., Wang, P., Zhuo, W., and Yang, M. (2019). Cryo-EM structure of the mammalian ATP synthase tetramer bound with inhibitory protein IF1. Science *364*, 1068–1075.

Guo, H., Bueler, S.A., and Rubinstein, J.L. (2017). Atomic model for the dimeric FO region of mitochondrial ATP synthase. Science *358*, 936–940.

Hahn, A., Parey, K., Bublitz, M., Mills, D.J., Zickermann, V., Vonck, J., Kühlbrandt, W., and Meier, T. (2016). Structure of a Complete ATP Synthase Dimer Reveals the Molecular Basis of Inner Mitochondrial Membrane Morphology. Mol. Cell *63*, 445–456.

Hahn, A., Vonck, J., Mills, D.J., Meier, T., and Kühlbrandt, W. (2018). Structure, mechanism, and regulation of the chloroplast ATP synthase. Science *360*, eaat4318.

He, J., Carroll, J., Ding, S., Fearnley, I.M., and Walker, J.E. (2017a). Permeability transition in human mitochondria persists in the absence of peripheral stalk subunits of ATP synthase. Proc. Natl. Acad. Sci. U.S.A. *114*, 9086–9091.

He, J., Ford, H.C., Carroll, J., Ding, S., Fearnley, I.M., and Walker, J.E. (2017b). Persistence of the mitochondrial permeability transition in the absence of subunit c of human ATP synthase. Proc. Natl. Acad. Sci. U.S.A. *114*, 3409–3414.

Jonckheere, A.I., Smeitink, J.A.M., and Rodenburg, R.J.T. (2012). Mitochondrial ATP synthase: architecture, function and pathology. J. Inherit. Metab. Dis. *35*, 211–225.

Junge, W., Lill, H., and Engelbrecht, S. (1997). ATP synthase: An electrochemical transducer with rotatory mechanics. Trends in Biochemical Sciences *22*, 420–423.

Junge, W., Sielaff, H., and Engelbrecht, S. (2009). Torque generation and elastic power transmission in the rotary F(O)F(1)-ATPase. Nature *459*, 364–370.

Karch, J., Bround, M.J., Khalil, H., Sargent, M.A., Latchman, N., Terada, N., Peixoto, P.M., and Molkentin, J.D. (2019). Inhibition of mitochondrial permeability transition by deletion of the ANT family and CypD. Sci Adv *5*, eaaw4597.

Klusch, N., Murphy, B.J., Mills, D.J., Yildiz, Ö., and Kühlbrandt, W. (2017). Structural basis of proton translocation and force generation in mitochondrial ATP synthase. Elife *6*, e33274.

Kucharczyk, R., Rak, M., and di Rago, J.-P. (2009). Biochemical consequences in yeast of the human mitochondrial DNA 8993T>C mutation in the ATPase6 gene found in NARP/MILS patients. Biochim. Biophys. Acta *1793*, 817–824.

Kucharczyk, R., Dautant, A., Godard, F., Tribouillard-Tanvier, D., and di Rago, J.-P. (2019). Functional investigation of an universally conserved leucine residue in subunit a of ATP synthase targeted by the pathogenic m.9176 T>G mutation. Biochim Biophys Acta Bioenerg *1860*, 52–59.

Kühlbrandt, W. (2019). Structure and Mechanisms of F-Type ATP Synthases. Annu. Rev. Biochem. *88*, 515–549.

Kühlbrandt, W., and Davies, K.M. (2016). Rotary ATPases: A New Twist to an Ancient Machine. Trends Biochem. Sci. *41*, 106–116.

Mitome, N., Ono, S., Sato, H., Suzuki, T., Sone, N., and Yoshida, M. (2010). Essential arginine residue of the F(o)-a subunit in F(o)F(1)-ATP synthase has a role to prevent the proton shortcut without c-ring rotation in the F(o) proton channel. Biochem. J. *430*, 171–177.

Mnatsakanyan, N., Llaguno, M.C., Yang, Y., Yan, Y., Weber, J., Sigworth, F.J., and Jonas, E.A. (2019). A mitochondrial megachannel resides in monomeric F1FO ATP synthase. Nat Commun *10*, 5823.

Morciano, G., Preti, D., Pedriali, G., Aquila, G., Missiroli, S., Fantinati, A., Caroccia, N., Pacifico, S., Bonora, M., Talarico, A., et al. (2018). Discovery of Novel 1,3,8-Triazaspiro[4.5]decane Derivatives That Target the c Subunit of F1/FO-Adenosine Triphosphate (ATP) Synthase for the Treatment of Reperfusion Damage in Myocardial Infarction. J. Med. Chem. *61*, 7131–7143.

Moro, L. (2019). Mitochondrial Dysfunction in Aging and Cancer. J Clin Med *8*.

Muench, S.P., Trinick, J., and Harrison, M.A. (2011). Structural divergence of the rotary ATPases. Q. Rev. Biophys. *44*, 311–356.

Mühleip, A.W., Joos, F., Wigge, C., Frangakis, A.S., Kühlbrandt, W., and Davies, K.M. (2016). Helical arrays of U-shaped ATP synthase dimers form tubular cristae in ciliate mitochondria. Proc. Natl. Acad. Sci. U.S.A. *113*, 8442–8447.

Mühleip, A.W., Dewar, C.E., Schnaufer, A., Kühlbrandt, W., and Davies, K.M. (2017). In situ structure of trypanosomal ATP synthase dimer reveals a unique arrangement of catalytic subunits. Proc. Natl. Acad. Sci. U.S.A. *114*, 992–997.

Murataliev, M.B., and Boyer, P.D. (1992). The mechanism of stimulation of MgATPase activity of chloroplast F1-ATPase by non-catalytic adenine-nucleotide binding. Acceleration of the ATP-dependent release of inhibitory ADP from a catalytic site. Eur. J. Biochem. *209*, 681–687.

Murphy, B.J., Klusch, N., Langer, J., Mills, D.J., Yildiz, Ö., and Kühlbrandt, W. (2019). Rotary substates of mitochondrial ATP synthase reveal the basis of flexible F1-Fo coupling. Science *364*.

Nakamura, J., Fujikawa, M., and Yoshida, M. (2013). IF1, a natural inhibitor of mitochondrial ATP synthase, is not essential for the normal growth and breeding of mice. Biosci. Rep. *33*.

Neginskaya, M.A., Solesio, M.E., Berezhnaya, E.V., Amodeo, G.F., Mnatsakanyan, N., Jonas, E.A., and Pavlov, E.V. (2019). ATP Synthase C-Subunit-Deficient Mitochondria Have a Small Cyclosporine A-Sensitive Channel, but Lack the Permeability Transition Pore. Cell Rep *26*, 11-17.e2.

Nesci, S. (2018). A Lethal Channel between the ATP Synthase Monomers. Trends Biochem. Sci. *43*, 311–313.

Nesci, S., and Pagliarani, A. (2019). Emerging Roles for the Mitochondrial ATP Synthase Supercomplexes. Trends Biochem. Sci. *44*, 821–823.

Nesci, S., Ventrella, V., Trombetti, F., Pirini, M., and Pagliarani, A. (2013). Mussel and mammalian ATP synthase share the same bioenergetic cost of ATP. J. Bioenerg. Biomembr. *45*, 289–300.

Nesci, S., Trombetti, F., Ventrella, V., and Pagliarani, A. (2015). Opposite rotation directions in the synthesis and hydrolysis of ATP by the ATP synthase: hints from a subunit asymmetry. J. Membr. Biol. *248*, 163–169.

Nesci, S., Trombetti, F., Ventrella, V., and Pagliarani, A. (2016). The c-Ring of the F1FO-ATP Synthase: Facts and Perspectives. J. Membr. Biol. *249*, 11–21.

Nesci, S., Trombetti, F., Ventrella, V., and Pagliarani, A. (2018). From the Ca2+-activated F1FO-ATPase to the mitochondrial permeability transition pore: an overview. Biochimie *152*, 85–93.

Niedzwiecka, K., Tisi, R., Penna, S., Lichocka, M., Plochocka, D., and Kucharczyk, R. (2018). Two mutations in mitochondrial ATP6 gene of ATP synthase, related to human cancer, affect ROS, calcium homeostasis and mitochondrial permeability transition in yeast. Biochim. Biophys. Acta *1865*, 117–131.

Niedzwiecka, K., Baranowska, E., Panja, C., and Kucharczyk, R. (2020). ATP Synthase Subunit a Supports Permeability Transition in Yeast Lacking Dimerization Subunits and Modulates yPTP Conductance. Cell. Physiol. Biochem. *54*, 211–229.

Niu, Y., Moghimyfiroozabad, S., Safaie, S., Yang, Y., Jonas, E.A., and Alavian, K.N. (2017). Phylogenetic Profiling of Mitochondrial Proteins and Integration Analysis of Bacterial Transcription Units Suggest Evolution of F1Fo ATP Synthase from Multiple Modules. J. Mol. Evol. *85*, 219–233.

Okuno, D., Iino, R., and Noji, H. (2011). Rotation and structure of FoF1-ATP synthase. J. Biochem. *149*, 655–664.

Paradies, G., Paradies, V., Ruggiero, F.M., and Petrosillo, G. (2013). Changes in the mitochondrial permeability transition pore in aging and age-associated diseases. Mech. Ageing Dev. *134*, 1–9.

Paumard, P., Vaillier, J., Coulary, B., Schaeffer, J., Soubannier, V., Mueller, D.M., Brèthes, D., di Rago, J.-P., and Velours, J. (2002). The ATP synthase is involved in generating mitochondrial cristae morphology. EMBO J. *21*, 221–230.

Peter, B.J., Kent, H.M., Mills, I.G., Vallis, Y., Butler, P.J.G., Evans, P.R., and McMahon, H.T. (2004). BAR domains as sensors of membrane curvature: the amphiphysin BAR structure. Science *303*, 495–499.

Pogoryelov, D., Krah, A., Langer, J.D., Yildiz, Ö., Faraldo-Gómez, J.D., and Meier, T. (2010). Microscopic rotary mechanism of ion translocation in the F(o) complex of ATP synthases. Nat. Chem. Biol. *6*, 891–899.

Pogoryelov, D., Klyszejko, A.L., Krasnoselska, G.O., Heller, E.-M., Leone, V., Langer, J.D., Vonck, J., Müller, D.J., Faraldo-Gómez, J.D., and Meier, T. (2012). Engineering rotor ring stoichiometries in the ATP synthase. Proc. Natl. Acad. Sci. U.S.A. *109*, E1599-1608.

Schmidt, T., Situ, A.J., and Ulmer, T.S. (2016). Structural and thermodynamic basis of proline-induced transmembrane complex stabilization. Sci Rep *6*, 29809.

Sgarbi, G., Baracca, A., Lenaz, G., Valentino, L.M., Carelli, V., and Solaini, G. (2006). Inefficient coupling between proton transport and ATP synthesis may be the pathogenic mechanism for NARP and Leigh syndrome resulting from the T8993G mutation in mtDNA. Biochem. J. *395*, 493–500.

Skoczeń, N., Dautant, A., Binko, K., Godard, F., Bouhier, M., Su, X., Lasserre, J.-P., Giraud, M.-F., Tribouillard-Tanvier, D., Chen, H., et al. (2018). Molecular basis of diseases caused by the mtDNA mutation m.8969G>A in the subunit a of ATP synthase. Biochim. Biophys. Acta *1859*, 602–611.

Solaini, G., Harris, D.A., Lenaz, G., Sgarbi, G., and Baracca, A. (2008). The study of the pathogenic mechanism of mitochondrial diseases provides information on basic bioenergetics. Biochim. Biophys. Acta *1777*, 941–945.

Song, J., Pfanner, N., and Becker, T. (2018). Assembling the mitochondrial ATP synthase. Proc. Natl. Acad. Sci. U.S.A. *115*, 2850–2852.

Srivastava, A.P., Luo, M., Zhou, W., Symersky, J., Bai, D., Chambers, M.G., Faraldo-Gómez, J.D., Liao, M., and Mueller, D.M. (2018). High-resolution cryo-EM analysis of the yeast ATP synthase in a lipid membrane. Science *360*, eaas9699.

Strauss, M., Hofhaus, G., Schröder, R.R., and Kühlbrandt, W. (2008). Dimer ribbons of ATP synthase shape the inner mitochondrial membrane. EMBO J. *27*, 1154–1160.

Suzuki, T., Tanaka, K., Wakabayashi, C., Saita, E., and Yoshida, M. (2014). Chemomechanical coupling of human mitochondrial F1-ATPase motor. Nat. Chem. Biol. *10*, 930–936.

Symersky, J., Pagadala, V., Osowski, D., Krah, A., Meier, T., Faraldo-Gómez, J.D., and Mueller, D.M. (2012). Structure of the c(10) ring of the yeast mitochondrial ATP synthase in the open conformation. Nat. Struct. Mol. Biol. *19*, 485–491, S1.

Szabo, I., and Zoratti, M. (2014). Mitochondrial channels: ion fluxes and more. Physiol. Rev. *94*, 519–608.

Trounce, I., Neill, S., and Wallace, D.C. (1994). Cytoplasmic transfer of the mtDNA nt 8993 T-->G (ATP6) point mutation associated with Leigh syndrome into mtDNA-less cells demonstrates cosegregation with a decrease in state III respiration and ADP/O ratio. Proc. Natl. Acad. Sci. U.S.A. *91*, 8334–8338.

Urbani, A., Giorgio, V., Carrer, A., Franchin, C., Arrigoni, G., Jiko, C., Abe, K., Maeda, S., Shinzawa-Itoh, K., Bogers, J.F.M., et al. (2019). Purified F-ATP synthase forms a Ca2+-dependent high-conductance channel matching the mitochondrial permeability transition pore. Nat Commun *10*, 4341.

Uziel, G., Moroni, I., Lamantea, E., Fratta, G.M., Ciceri, E., Carrara, F., and Zeviani, M. (1997). Mitochondrial disease associated with the T8993G mutation of the mitochondrial ATPase 6 gene: a clinical, biochemical, and molecular study in six families. J. Neurol. Neurosurg. Psychiatry *63*, 16–22.

Vinogradov, A.D. (2019). New Perspective on the Reversibility of ATP Synthesis and Hydrolysis by Fo·F1-ATP Synthase (Hydrolase). Biochemistry Moscow *84*, 1247–1255.

Wolf, D.M., Segawa, M., Kondadi, A.K., Anand, R., Bailey, S.T., Reichert, A.S., van der Bliek, A.M., Shackelford, D.B., Liesa, M., and Shirihai, O.S. (2019). Individual cristae within the same mitochondrion display different membrane potentials and are functionally independent. EMBO J. e101056.

Xu, T., Pagadala, V., and Mueller, D.M. (2015). Understanding structure, function, and mutations in the mitochondrial ATP synthase. Microb Cell *2*, 105–125.

Yoshida, M., Muneyuki, E., and Hisabori, T. (2001). ATP synthase--a marvellous rotary engine of the cell. Nat. Rev. Mol. Cell Biol. *2*, 669–677.

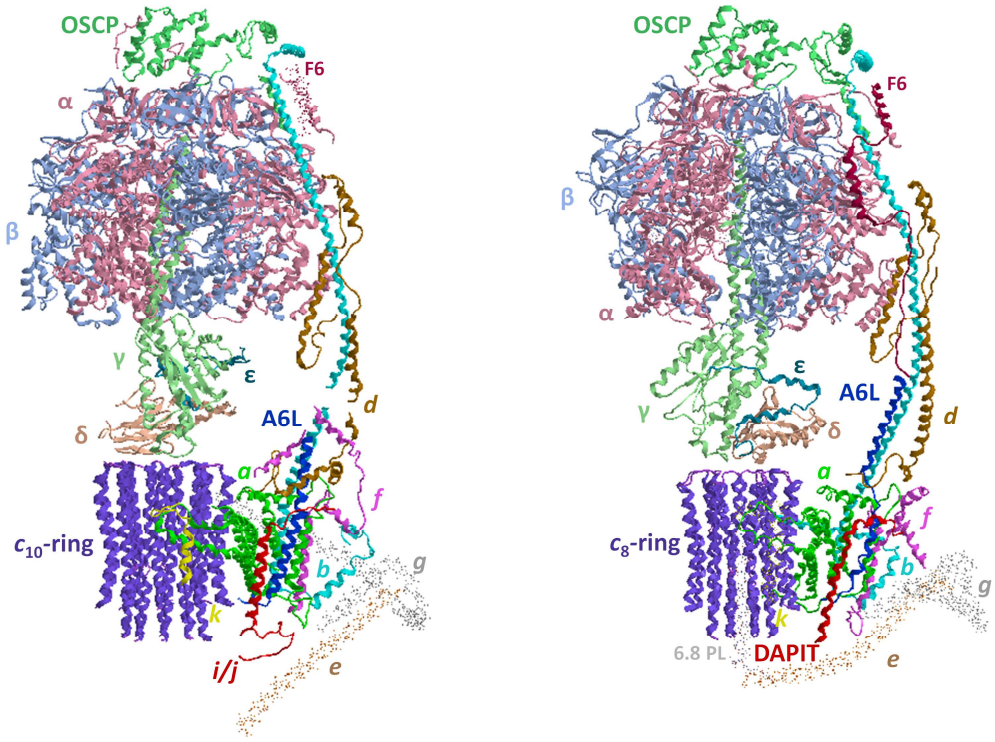

Figure 1. Overall structure of F_1F_O-ATP synthase monomers in yeast and mammalian mitochondria. Enzyme subunits are drawn as ribbon representations obtained from modified PDB ID codes: 6B8H (Guo et al., 2017) and 6J5J (Gu et al., 2019) of yeast (left panel) and mammalian (right panel) F_1F_O-ATP synthase monomers, respectively. According to Chem3D software, subunits with unknown amino acid sequence are drawn as ball and stick models.

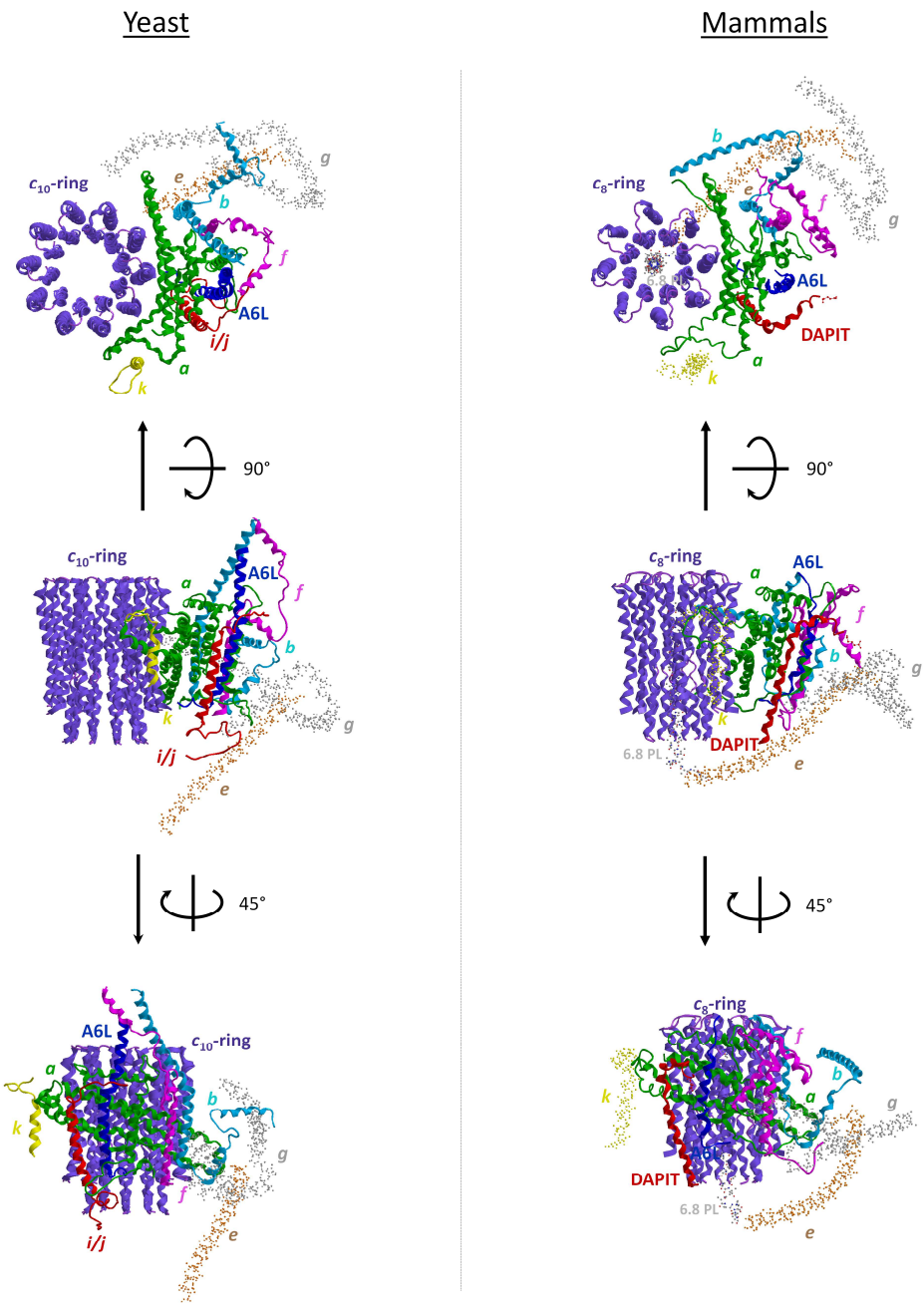

Figure 2. F_O domain structure in yeast and mammalian mitochondria. The membrane subunit composition and their molecular arrangement are shown as ribbon representations obtained by modifying PDB ID codes 6B2Z (yeast) (Guo et al., 2017) and 6J54 (mammal) (Gu et al., 2019). Yeast and mammalian F_O domains, as viewed from different sides, are shown on the left and right panel, respectively. According to Chem3D software, subunits with unknown amino acid sequence are drawn as ball and stick models.

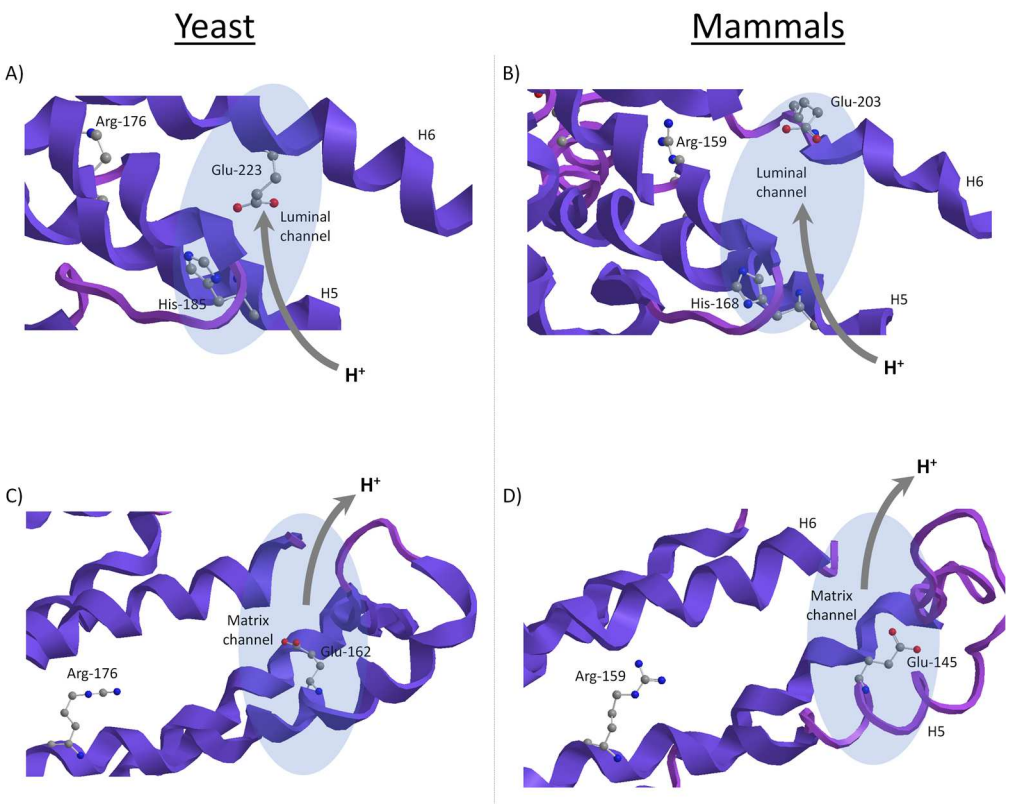

Figure 3. Crucial amino acids for H^+ pathway in the *a* subunit. In A) and B) the lumen H^+-pathway (viewed with *a* subunit between the observer and the *c*-ring), in C) and D) the matrix H^+-pathway (viewed with the *c*-ring between the observer and the *a* subunit), in yeast (on the left) and mammalian mitochondria (on the right), respectively. The amino acid side chains that are involved in the H^+ pathway are shown as ball and stick models. The light-blue oval shape indicates the half-channel region. H5 and H6 indicate the α-helices of *a* subunit. The *a* subunits in yeast and mammalian F_1F_O-ATPases are drawn by modifying PDB ID codes 6B2Z (Guo et al., 2017) and 6J5A (Gu et al., 2019), respectively.